

## VLBI-DERIVED TRIGONOMETRIC PARALLAX AND PROPER MOTION OF PSR B2021+51

R. M. CAMPBELL,<sup>1,2</sup> N. BARTEL,<sup>3</sup> I. I. SHAPIRO,<sup>1</sup> M. I. RATNER,<sup>1</sup> R. J. CAPPALLO,<sup>4</sup> A. R. WHITNEY,<sup>4</sup> AND N. PUTNAM<sup>5</sup>

Received 1995 December 11; accepted 1996 February 13

### ABSTRACT

We present the first results from a long-term program to measure the trigonometric parallaxes and proper motions of a set of pulsars using VLBI. We obtained these results for PSR B2021+51 from four sessions of S-band observations of the pulsar and associated reference sources. We estimate a parallax of  $0.95 \pm 0.37$  mas, a proper motion of  $\mu_\alpha = -8.11 \pm 0.24$  mas yr<sup>-1</sup> and  $\mu_\delta = +13.41 \pm 0.25$  mas yr<sup>-1</sup>, and a position at epoch 1992.723 of  $\alpha = 20^{\text{h}}22^{\text{m}}49^{\text{s}}.87031 \pm 0^{\text{s}}.00004$  and  $\delta = 51^{\circ}54'50''.2913 \pm 0''.0003$  (all J2000). Our parallax estimate implies an average electron density of  $0.021 \pm 0.008$  cm<sup>-3</sup> along the line of sight to the pulsar. We also effectively rule out a physical association with the supernova remnant HB 21.

*Subject headings:* astrometry — pulsars: individual (PSR B2021+51) — techniques: interferometric

### 1. INTRODUCTION

Interleaved VLBI phase-delay observations of two or more compact radio sources that lie near each other on the plane of the sky can be used to determine their relative positions with submilliarcsecond uncertainty. Specifically, a series of observations, well spread throughout the seasons, of a system comprising a pulsar and one or more extragalactic reference sources can yield the position, proper motion ( $\mu$ ), and trigonometric parallax ( $\pi$ ) of the pulsar. The parallax yields a model-independent distance. In principle, such results can be used in the following ways: (1) distances, along with independent dispersion measures, can yield the electron density,  $n_e$ , integrated along the line of sight to each of the various pulsars so studied, which would provide checks on models of the Galactic  $n_e$  distribution (e.g., Lyne, Manchester, & Taylor 1985; Taylor & Cordes 1993); (2) distances, along with independent measures of the angular diameters of pulsars' scattering disks at two or more frequencies, can determine similarly integrated values for the coefficient and exponent of the power-law spectrum for the  $n_e$  spatial fluctuations, which may provide insights into the mechanisms driving turbulence in the ISM (e.g., Gwinn, Bartel, & Cordes 1993); (3) distances and proper motions, along with independent age estimates, can provide bounds on the birthplaces of pulsars; and (4) positions, along with independent pulse time-of-arrival data, can contribute toward a tie between the extragalactic (Earth-rotation-based) and dynamic (Earth-orbit-based) reference frames (e.g., Shapiro & Knight 1970).

To date, radio interferometry has yielded nonzero trigonometric parallax determinations for four pulsars: PSR B1451–68,  $\pi = 2.2 \pm 0.3$  mas (Bailes et al. 1990); PSR B0823+26,  $\pi = 2.8 \pm 0.6$  mas; PSR B0950+08,  $\pi = 7.9 \pm 0.8$  mas (both from Gwinn et al. 1986); and PSR B1929+10, with the discrepant results  $\pi = 21.5 \pm 0.3$  mas (Salter, Lyne, & Anderson 1979) and  $\pi < 4$  mas (Backer & Sramek 1982). Accurate pulsar proper motion and distances may also be

determined through timing analysis, especially for millisecond pulsars (e.g., Ryba & Taylor 1991; Bell & Bailes 1996). We have begun a long-term program to measure with VLBI the trigonometric parallaxes of 15 pulsars, which were originally selected based on their brightness at S-band frequencies and their declinations, the latter for providing long durations of mutual visibility from Northern Hemisphere antennas. In the course of our four observing sessions since 1991 July, we have obtained useful data from at least one session for each of nine pulsars. This Letter focuses on PSR B2021+51, the first of these pulsars for which we have analyzed four sessions of observations. We will briefly describe the general tactics of our program, summarize the observations and astrometric analysis pertaining to PSR B2021+51, and present the resulting parallax solution. Campbell (1995) provides a more thorough description of the parallax program, the constituent observations, and the steps in the data reduction.

### 2. OBSERVATIONS AND ANALYSIS

We observed at S band ( $\nu_0 = 2.218$  GHz) as a compromise between (1) the desire for smaller fringe spacings and for minimal ionospheric phase perturbations, each of which pushes us toward higher frequencies, and (2) the pulsars' steep spectra, the desire for shorter integration times to enable faster switching, and the possibility of finding reference sources within the beam of each antenna, which together push us toward lower frequencies. The pulsars' faintness at higher frequencies precludes standard dual frequency astrometric observations, which would have provided straightforward ionospheric corrections. With only one frequency band available, such corrections could be estimated by using group and phase delays, which are oppositely affected by the ionosphere (see, e.g., Bartel et al. 1985a). However, this technique provides only limited accuracy and would only be useful if close reference sources could not be found. The selection of reference sources thus becomes critical; we want the pulsar and its reference source(s) to be as close as possible in direction and in epoch of observation to minimize the effects of any spatial or temporal variations in refractivity affecting the propagation paths from the different sources to each antenna. In addition, the use of two extragalactic reference sources per pulsar provides a means to check the stability of our astrometric solution across the observing sessions; we would expect to see

<sup>1</sup> Harvard-Smithsonian Center for Astrophysics, 60 Garden Street, Cambridge, MA 02138.

<sup>2</sup> Present address: Phillips Laboratory/GPIM, 29 Randolph Road, Hanscom AFB, MA 01731; campbellr@plh.af.mil.

<sup>3</sup> Department of Physics and Astronomy, York University, 4700 Keele Street, North York, Ontario M3J 1P3, Canada.

<sup>4</sup> Haystack Observatory, Off Route 40, Westford, MA 01866.

<sup>5</sup> Department of Physics, Brown University, Providence, RI 02912.

TABLE 1  
JOURNAL OF OBSERVATIONS

Observing Session	Stations <sup>a</sup>	$t_{\text{PSR}}/t_{\text{tot}}^b$ (hr)
1991 Jul 27.....	L-E-C-G-R-A	3/3
1992 May 9.....	L-NI-Kp-A	1/5.7
1993 Mar 15.....	NI-Pt-Kp-Br-Ov	4/4.5
1993 Oct 5.....	Hn-NI-Pt-Kp-Br-Ov	2/6

<sup>a</sup> Station abbreviations (two-letter abbreviations denote VLBA stations): L—Medicina, E—Westford, C—Algonquin, G—Green Bank 26 m (85'), R—Richmond, A—Fairbanks, Hn—Hancock, NI—North Liberty, Pt—Pie Town, Kp—Kitt Peak, Br—Brewster, and Ov—Owens Valley.

<sup>b</sup> For each session,  $t_{\text{PSR}}$  is the duration of useful pulsar detections on the most sensitive baseline and  $t_{\text{tot}}$  is the total duration of the observations.

no proper motion between the two extragalactic sources on the timescale of a few years. Initially, we selected reference sources from the JPL VLBI survey (Preston et al. 1985). As part of our first session (see Table 1), we observed about 60 new reference-source candidates, drawn primarily from the 87GB survey (Gregory & Condon 1991). We observed each candidate for about 6.5 minutes, detecting about one-third of them. For PSR B2021+51 we used 2037+51 (i.e., 3C 418: 2?5 away from the pulsar,  $z \sim 1.7$ ) as the fixed reference source in all observing sessions, and added 2019+51 (0?3 away), starting with the second observing session, after having detected it in the candidate search. The cycle time to observe the three sources in sequence was typically  $8^m 20^s$ .

For each observing session, we need to determine the proper integral number of cycles of phase to “connect” the phase delays of all the individual scans of each source (see, e.g., Reisz et al. 1973). We found that a network of about six stations observing for about 6 hr provides sufficient ( $u$ ,  $v$ ) coverage and enough closure constraints to determine the structure phases for the reference sources, and to reliably phase-connect the data from each source. However, one must always be alert for the subtle error in which, for a given station in a given session, the connected phase delays of all the scans of one source are inconsistent with those of another source by some integral number of cycles of phase.

In the first session, we used the Mk IIIA recording system (Rogers et al. 1983) in mode A (14 video channels, 2 MHz upper and lower sidebands). With the later inclusion of VLBA stations, which have only eight independent video converters, we shifted to Mk IIIA mode B, recording at double speed in order to preserve the total recorded bandwidth (seven video channels, 4 MHz upper and lower sidebands). For all observations, we recorded right-circular polarization. The data were correlated on the Haystack Mk IIIA correlator (Whitney 1988); we used rectangular gating in processing the pulsar scans. We determined the optimal gate parameters (width and central phase) empirically for each session. Such gating increases the signal-to-noise ratio of the pulsar scans by the inverse square root of the pulsar’s duty cycle, i.e., by factors of 3–5 (see, e.g., Bartel et al. 1985b).

Table 1 provides a journal of the PSR B2021+51 observations. In the 1992 May session, errors made in the implementation of our nonstandard configuration at two stations resulted in only a four-station network. In the 1993 March session, a mechanical problem at a VLBA antenna left only a five-station network. In general, the correlation amplitudes of PSR B2021+51 exhibited systematic fluctuations characteris-

tic of diffractive interstellar scattering, which caused the duration of pulsar detectability to be shorter than the total span of observations. We ruled out poorly phased gating as a cause of such amplitude variability by independently determining gate parameters for several observations within each session, thereby confirming that there was no drift of the central phase of the optimal gate with time.

We used the International Earth Rotation Service combined solution (IERS 1993) to express source coordinates, station coordinates, and Earth-orientation parameters consistently. This solution comprises the IERS Celestial Reference Frame, through which we obtained the coordinates of 2037+51; the IERS Terrestrial Reference Frame, through which we obtained station coordinates at epoch 1988.0 and station velocities with which to determine station coordinates at other epochs; and a file containing polar motion, UT1-UTC, and nutation values tabulated at daily intervals. For each session, we used the Caltech VLBI package (Shepard, Pearson, & Taylor 1994) to map the reference sources, and we corrected their phase delays for the structure phases derived from the resulting CLEAN models. Our maps of 2037+51 are consistent with the MERLIN European VLBI Network (EVN) maps of Muxlow & Garrington (1991) and Muxlow (1993), although we resolve out the astrophysically interesting region where the jet bends through more than  $90^\circ$ . On the other hand, 2019+51 appears unresolved to our networks.

Following phase connection, we estimated the positions of the pulsar and the second reference source from the resulting phase delays and differenced phase delays using a linearized, weighted least-squares algorithm (Robertson 1975). To avoid the effects of linear dependencies among the undifferenced phase delays and the differenced phase delays that are formed from them, we included undifferenced data only from 2037+51 in our analysis. The differenced phase delays for each pair of sources should be insensitive to refractivity variations on angular scales larger than the separation of the sources and on timescales longer than the cycle time. To incorporate this decreased sensitivity to refractivity effects, we increased the relative weight of the differenced phase delays for each pair of sources. Campbell (1995) investigated the sensitivity of the estimated source positions to the specific form of this relative weighting; in the present analysis, we took the weighting factor for each pair to be the inverse square root of the angular separation of the two sources forming the pair.

Given the previously mentioned possibility of an ambiguity offset between all the phase delays for baselines involving a given station for one source with respect to the corresponding delays for another source, we introduced for each station a “constant clock offset” parameter (CCO) for each source. We initially treated the CCOs as free parameters; if each indeed represents such an ambiguity error for a given source, each will be an integral multiple of an ambiguity time (i.e., will equal  $n/v_0$ , with  $n$  an integer). We have found that values of  $n$  corresponding to these CCO estimates fall within 0.15 of an integer after a small number of iterations. We estimated source positions with respect to that of the fixed reference source, with the CCO parameters fixed at their nearest integral ambiguity time. For sessions in which we observe three sources (i.e., all but the first session), consecutive differenced phase delays “share” a common undifferenced phase delay; to investigate the effects of any resulting correlations, we created two independent subsets for each session by omitting differenced data at alternate observing times. The

TABLE 2

POSITION, PROPER MOTION, AND PARALLAX FOR PSR B2021+51

Parameter <sup>a</sup>	Value	$\alpha^b$	$\delta^b$	$\mu_\alpha$	$\mu_\delta$
$\mu_\alpha$ (mas yr <sup>-1</sup> )	$-8.11 \pm 0.24$	0.18	-0.54	...	...
$\mu_\delta$ (mas yr <sup>-1</sup> )	$13.41 \pm 0.25$	-0.07	-0.42	0.15	...
$\pi$ (mas)	$0.95 \pm 0.37$	0.30	-0.62	0.46	0.66

NOTE.—The last four columns list the correlations among the parameter estimates.

<sup>a</sup> The reference epoch for the estimation of position, proper motion, and parallax is 1992.723.

<sup>b</sup> The estimated position (J2000) of the pulsar at the reference epoch is  $\alpha = 20^{\text{h}}22^{\text{m}}49^{\text{s}}.87031 \pm 0^{\text{s}}.00004$ ,  $\delta = 51^{\circ}54'50''.2913 \pm 0''.0003$ , with a correlation between the estimates of the two coordinates of  $-0.37$ . The position of the fixed reference source 2037+51, taken from IERS (1993), is  $\alpha = 20^{\text{h}}38^{\text{m}}37^{\text{s}}.034766 \pm 0^{\text{s}}.000016$ ,  $\delta = 51^{\circ}19'12''.66264 \pm 0''.00013$ .

resulting position estimates were not significantly different from those obtained through analysis using all of the differenced data, although the standard errors increased somewhat less than the factor that would result solely from considerations of the number and relative weights of the data. The standard errors in the estimated source positions should reflect our sensitivity to the estimation of the integral ambiguity-time CCO parameters and, for sessions including three sources, to any correlations among the differenced data. To be conservative, we used the statistical standard deviations from analysis in which we treated the CCOs as free parameters, scaled to obtain a reduced  $\chi^2$  of unity; for sessions with three sources, we used the mean of such values from analyses of the two alternating data subsets, normalized by a factor of  $2^{-1/2}$ .

The analysis of the data from the “outer” observing sessions (i.e., 1991 July and 1993 October) proceeded along the above lines without significant complication, and yielded reliable position estimates for the pulsar (and for 2019+51 in 1993 October). The 1992 May session suffered from the loss of two stations, the underestimation of the integration time needed for each scan of the new reference source 2019+51, and the detection of the pulsar for only about 1 hr. The resulting dearth of closure triangles and surfeit of sizable gaps in the data rendered the phase connection more uncertain, but we were able to find a solution that resulted in no significant proper motion for 2019+51 between 1992 May and 1993 October:  $\mu_\alpha = +0.1 \pm 0.5$  mas yr<sup>-1</sup> and  $\mu_\delta = +0.06 \pm 0.22$  mas yr<sup>-1</sup>, where  $\mu_\alpha \equiv \dot{\alpha} \cos \delta$  and  $\mu_\delta \equiv \dot{\delta}$ . We learned during data analysis that the 1993 March observing session coincided with a brief period of unusually strong geomagnetic disturbance (Foster 1994). The effects of this activity on the ionosphere and, hence, on our data led us to conclude that for this session (1) use of the undifferenced phase delays precluded a reliable phase connection, and (2) 2037+51 was too far from the pulsar on the plane of the sky to provide reliable astrometry as the sole fixed reference source. Therefore, we used only the differenced phase delays to estimate the pulsar position with respect to the (fixed) positions of 2037+51 and 2019+51, the latter at its estimated 1993 October position.

### 3. RESULTS AND INTERPRETATION

We obtained the parallax, proper motion, and position of the pulsar by weighted least-squares analysis of the estimated pulsar positions ( $\alpha$ ,  $\delta$ ) from the four sessions, including the estimated correlation between  $\alpha$  and  $\delta$  at each session. Table 2 summarizes the position, proper-motion, and parallax results from this analysis. Figure 1 shows the pulsar’s estimated

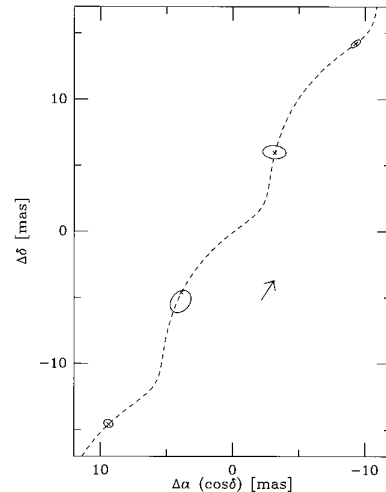


FIG. 1.—PSR B2021+51 positions and  $1\sigma$  error ellipses, with a superposed curve representing the modeled pulsar track across the plane of the sky, as calculated from the estimated parameters in Table 2. The origin represents the calculated pulsar position at the reference epoch (1992.723). A cross denotes the calculated pulsar position at the epoch of each observing session (see Table 1). North is up, and east is to the left; the direction of motion is toward the north-northwest.

position and one standard deviation ( $1\sigma$ ) error ellipse at the epoch of each session, with a superposed curve representing the modeled pulsar track across the plane of the sky, calculated from the parameter estimates listed in Table 2. The previously discussed problems with our two “middle” sessions resulted in large uncertainties in the position estimates for these two sessions, and they are mainly responsible for the large standard error,  $\sigma_\pi$ , in the estimated parallax. Use of an  $F$ -test (e.g., Bevington 1969) to compare models including and excluding parallax as a parameter shows that we can reject the null hypothesis, the exclusion of the parallax parameter, at about a 96% confidence level. Figure 2 compares our proper-motion estimate with previous ones. Our disagreement with the Lyne, Anderson, & Salter (1982) value is at an approximately  $3\sigma$  level; proper-motion differences on a similar scale have also resulted for other pulsars in their sample that have been the object of subsequent interferometric observation (e.g., Gwinn et al. 1986; Campbell 1995). These disagreements may stem from the lower frequency of the Lyne et al. (1982) observations and the effects of structure in their reference sources, both of which are reflected in their measurement of apparent proper motion on the order of  $10$  mas yr<sup>-1</sup> between reference sources associated with the same pulsar.

Our estimated parallax corresponds to a distance of  $D = 1.1^{+0.7}_{-0.3}$  kpc. This value slightly favors the dispersion-based

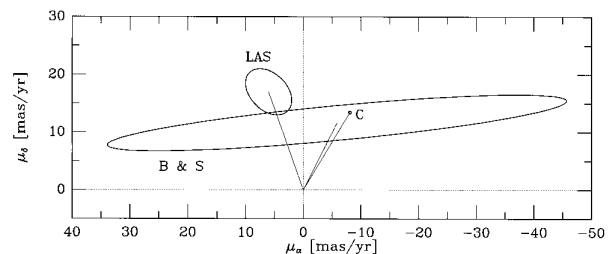


FIG. 2.—Proper-motion estimates and  $1\sigma$  error ellipses for PSR B2021+51 from this project (C), Lyne et al. (1982) (LAS), and Backer & Sramek (1981) (B & S).

distance derived from the Taylor & Cordes (1993)  $n_e$  model ( $D_{\text{dm}} = 1.22$  kpc) over that derived from the Lyne et al. (1985)  $n_e$  model ( $D_{\text{dm}} = 0.71$  kpc), where the dispersion measure of PSR B2021+51 is  $22.580 \text{ cm}^{-3} \text{ pc}$ . Our value of  $D$  yields a line-of-sight averaged electron density of  $n_e = 0.021 \pm 0.008 \text{ cm}^{-3}$ . Our distance and proper-motion estimates yield a transverse velocity for the pulsar in its own local standard of rest (LSR) of  $v_t = 95_{-27}^{+60} \text{ km s}^{-1}$ . In reducing the observed proper motion to the pulsar's LSR, we have used the Galactic rotation law from Brand (1986)— $(\Theta/\Theta_0) = 0.1121(R/R_0)^{0.4142} + 0.90262$ , with  $R_0 = 8.5$  kpc and  $\Theta_0 = 220 \text{ km s}^{-1}$ —and solar motion from Mihalas & Binney (1981, hereafter MB). We can also estimate the kinetic age,  $\tau_k$ , of the pulsar, i.e., the time it would have taken the pulsar to reach its current location above the Galactic plane ( $b = +8^\circ 4'$ ), given its velocity out of the plane and an assumed birthplace in the Galaxy. We performed a Monte Carlo analysis to incorporate our sensitivity to the observed parallax (characterized by a Gaussian distribution with a mean of  $\pi$  and a standard deviation of  $\sigma_\pi$ ), to the pulsar's unmeasured radial velocity ( $v_r$ , drawn from a zero-mean Gaussian distribution with a standard deviation of  $v_r/2^{1/2}$ ), and to the pulsar's birthplace with respect to the Galactic plane ( $z_0$ , drawn from a zero-mean exponential distribution with a scale height of 60 pc, i.e., that of OB stars [MB]). The resulting kinetic age is  $\tau_k = 2.6 \pm 1.3$  Myr, based on our use of  $10^5$  Monte Carlo trials and our rejection of individual  $\tau_k < 0$ . The bulk of the uncertainty in  $\tau_k$  arises from the range of allowed  $z_0$ ; if we set  $z_0 = 0$  in the Monte Carlo analysis, the kinetic age becomes  $2.4 \pm 0.4$  Myr. Our value of  $\tau_k$  is consistent with the pulsar's characteristic age ( $\tau_c \equiv P/2\dot{P} = 2.8$  Myr) and a decay timescale for neutron star magnetic fields greater than 2 Myr, including the case of no field decay at all (see, e.g., Fig. 7 of Harrison, Lyne, & Anderson 1993).

The current position of PSR B2021+51 is within  $3^\circ 7'$  on the sky of the supernova remnant HB 21 (G89.0+4.7). Previous distance estimates to HB 21 include 1.0–1.6 kpc (Leahy 1987, based on the  $\Sigma$ - $D$  relation) and  $800 \pm 70$  pc (Tatematsu et al. 1990, based on an inferred physical proximity of HB 21 to the

Cyg OB7 stellar association), both consistent with our distance estimate for the pulsar of  $1.1_{-0.3}^{+0.7}$  kpc. However, Leahy (1987) estimated the age of HB 21 to be 8–15 kyr, using models of SNR expansion into a three-component interstellar medium, while we find that use of our proper motion to follow the pulsar back through time places its point of closest approach on the sky to HB 21, about 700 kyr ago. We may, therefore, with some confidence rule out a physical connection between the two.

The amount and quality of our most recent data for this and other pulsars, collected with an exclusively VLBA array, as well as the ease of the phase connection, give us cause for optimism about the prospects of our pulsar parallax program. For PSR B2021+51, only a few additional sessions with similar data quality to 1993 October should yield a standard error in the estimated parallax of  $\sim 0.2$  mas. However, continued use of our current observational tactics would require the availability of gated-mode correlation on the new VLBA correlator in order to maintain our cycle times at  $\sim 8$  minutes; it is not clear that this correlator capability will be available by the next solar minimum, in 1996–1997, when ionospheric perturbations should also be at a minimum.

We thank the staffs of the participating observatories for supporting our experiments, notably Barry Clark, Tony Beasley, Wayne Cannon, Bill Petrachenko, and Joe Popelar. We especially recognize the Haystack correlator operations staff for ensuring expeditious processing of the 1993 October data. Operation of the Mk IIIA correlator at Haystack Observatory was funded by the NSF through the Northeast Radio Observatory Corporation. We gratefully acknowledge support from NASA grant NGT-50663 (R. M. C.), NSF grants AST89-02087 (N. B., R. M. C., and I. I. S.) and AST93-03527 (R. M. C. and I. I. S.), and the NSF Research Experiences for Undergraduates Program AST93-21943 (N. P.). Research at York University was partially supported by NSERC of Canada.

## REFERENCES

- Backer, D. C., & Sramek, R. A. 1981, in IAU Symp. 95, Pulsars, ed. W. Sieber & R. Wielebinski (Dordrecht: Reidel), 205  
 ———. 1982, *ApJ*, 260, 512  
 Bailes, M., Manchester, R. N., Kesteven, M. J., Norris, R. P., & Reynolds, J. E. 1990, *Nature*, 343, 240  
 Bartel, N., Ratner, M. I., Shapiro, I. I., Cappallo, R. J., Rogers, A. E. E., & Whitney, A. R. 1985a, *AJ*, 90, 318  
 ———. 1985b, *AJ*, 90, 2532  
 Bell, J. E., & Bailes, M. 1996, *ApJ*, 456, L33  
 Bevington, P. R. 1969, *Data Reduction and Error Analysis for the Physical Sciences* (New York: McGraw-Hill)  
 Brand, J. 1986, Ph.D. thesis, Univ. of Leiden  
 Campbell, R. M. 1995, Ph.D. thesis, Harvard Univ.  
 Foster, J. C. 1994, private communication  
 Gregory, P. C., & Condon, J. J. 1991, *ApJS*, 75, 1011  
 Gwinn, C. R., Bartel, N., & Cordes, J. M. 1993, *ApJ*, 410, 673  
 Gwinn, C. R., Taylor, J. H., Weisberg, J. M., & Rawley, L. A. 1986, *AJ*, 91, 338  
 Harrison, P. A., Lyne, A. G., & Anderson, B. 1993, *MNRAS*, 261, 113  
 International Earth Rotation Service (IERS). 1993, 1992 IERS Annu. Rep. (Paris: Obs. Paris)  
 Leahy, D. A. 1987, *MNRAS*, 238, 907  
 Lyne, A. G., Anderson, B., & Salter, M. J. 1982, *MNRAS*, 201, 503  
 Lyne, A. G., Manchester, R. N., & Taylor, J. H. 1985, *MNRAS*, 213, 613  
 Mihalas, D., & Binney, J. 1981, *Galactic Astronomy* (New York: Freeman) (MB)  
 Muxlow, T. W. B. 1993, in *Sub-arcsecond Radio Astronomy*, ed. R. J. Davis & R. S. Booth (Cambridge: Cambridge Univ. Press), 252  
 Muxlow, T. W. B., & Garrington, S. T. 1991, in *Beams and Jets in Astrophysics*, ed. P. A. Hughes (Cambridge: Cambridge Univ. Press), 52  
 Preston, R. A., Morabito, D. D., Williams, J. G., Faulkner, J., Jauncey, D. L., & Nicolson, G. D. 1985, *AJ*, 90, 1599  
 Reisz, A. C., Shapiro, I. I., Moran, J. M., Papadopoulos, G. D., Burke, B. F., Lo, K. Y., & Schwartz, P. R. 1973, *AJ*, 186, 537  
 Robertson, D. S. 1975, Ph.D. thesis, MIT  
 Rogers, A. E. E., et al. 1983, *Science*, 219, 51  
 Ryba, M. F., & Taylor, J. H. 1991, *ApJ*, 371, 739  
 Salter, M. J., Lyne, A. G., & Anderson, B. 1979, *Nature*, 280, 477  
 Shapiro, I. I., & Knight, C. A. 1970, in *Earthquake Displacement Fields and the Rotation of the Earth*, ed. L. Mansinha, D. E. Smylie, & A. E. Beck (Dordrecht: Reidel), 284  
 Shepard, M. C., Pearson, T. J., & Taylor, G. B. 1994, *BAAS*, 26, 987  
 Tatematsu, K., Fukui, Y., Landecker, T. L., & Roger, R. S. 1990, *A&A*, 237, 189  
 Taylor, J. H., & Cordes, J. M. 1993, *ApJ*, 411, 674  
 Whitney, A. R. 1988, in *Earth's Rotation and Reference Frames for Geodesy and Geodynamics*, ed. A. K. Babcock & G. A. Wilkins (Dordrecht: Kluwer), 439